

# Development and testing of a compartmentalized reaction network model for redox zones in contaminated aquifers

Robert H. Abrams and Keith Loague

Department of Geological and Environmental Sciences, Stanford University, Stanford, California

Douglas B. Kent

U.S. Geological Survey, Menlo Park, California

**Abstract.** The work reported here is the first part of a larger effort focused on efficient numerical simulation of redox zone development in contaminated aquifers. The sequential use of various electron acceptors, which is governed by the energy yield of each reaction, gives rise to redox zones. The large difference in energy yields between the various redox reactions leads to systems of equations that are extremely ill-conditioned. These equations are very difficult to solve, especially in the context of coupled fluid flow, solute transport, and geochemical simulations. We have developed a general, rational method to solve such systems where we focus on the dominant reactions, compartmentalizing them in a manner that is analogous to the redox zones that are often observed in the field. The compartmentalized approach allows us to easily solve a complex geochemical system as a function of time and energy yield, laying the foundation for our ongoing work in which we couple the reaction network, for the development of redox zones, to a model of subsurface fluid flow and solute transport. Our method (1) solves the numerical system without evoking a redox parameter, (2) improves the numerical stability of redox systems by choosing which compartment and thus which reaction network to use based upon the concentration ratios of key constituents, (3) simulates the development of redox zones as a function of time without the use of inhibition factors or switching functions, and (4) can reduce the number of transport equations that need to be solved in space and time. We show through the use of various model performance evaluation statistics that the appropriate compartment choice under different geochemical conditions leads to numerical solutions without significant error. The compartmentalized approach described here facilitates the next phase of this effort where we couple the redox zone reaction network to models of fluid flow and solute transport.

## 1. Introduction

The work described in this paper is the foundation of a larger, ongoing effort that focuses on process-based numerical simulation of the development of redox zones in contaminated aquifers; i.e., coupled modeling of fluid flow, solute transport, and geochemical reactions. In this study, we focus on the degradation of dissolved organic carbon, occurring via biogeochemical reactions, as the driving force for redox zone formation.

Redox reactions that describe organic carbon degradation must be viewed in both an inorganic and organic chemical framework. The process of biodegradation ultimately converts organic carbon to inorganic carbon and changes the oxidation state of many inorganic compounds. This occurs because the active microbes mediate oxidation/reduction (redox) reactions between organic carbon (electron donor) and various inorganic electron acceptors [Lovley *et al.*, 1994]. These redox reactions involve hydrogen ions; and thus they can affect *pH*. Most of these redox reactions also cause changes in carbonate alkalinity. Changes in the oxidation state of inorganic constituents can cause (1) anoxic conditions, (2) removal of undesir-

able inorganic contaminants (e.g., nitrate), (3) precipitation/dissolution of solid phases, and (4) changes in toxicity and mobility of many hazardous dissolved metals.

In many aquifers, electron acceptors such as oxygen, manganese oxides, and iron oxyhydroxides occur naturally. Electron acceptors such as nitrate, sulfate, and additional dissolved oxygen are introduced to aquifers via anthropogenic contamination and natural aquifer recharge. Other than natural sources, organic carbon is introduced into aquifers either in the aqueous phase or as a nonaqueous phase liquid which subsequently dissolves. Thus modeling organic carbon degradation in aquifers is a groundwater flow and solute transport problem in addition to an organic and inorganic chemistry problem.

### 1.1. Redox Zonation

The development of redox zones in aquifers has been discussed by many authors [Baedecker and Back, 1979a, b; Champ *et al.*, 1979; Edmunds *et al.*, 1982, 1984; Jackson and Patterson, 1982; Barcelona *et al.*, 1989; Lyngkilde and Christensen, 1992; Baedecker *et al.*, 1993; Bennett *et al.*, 1993; Eganhouse *et al.*, 1993; Cozzarelli *et al.*, 1994; Lovley *et al.*, 1994]. These studies show that up to five redox zones can develop: (1) zone of oxygen reduction, (2) zone of denitrification and manganese reduction, (3) zone of iron reduction, (4) zone of sulfate re-

Copyright 1998 by the American Geophysical Union.

Paper number 98WR00485.  
0043-1397/98/98WR-00485\$09.00

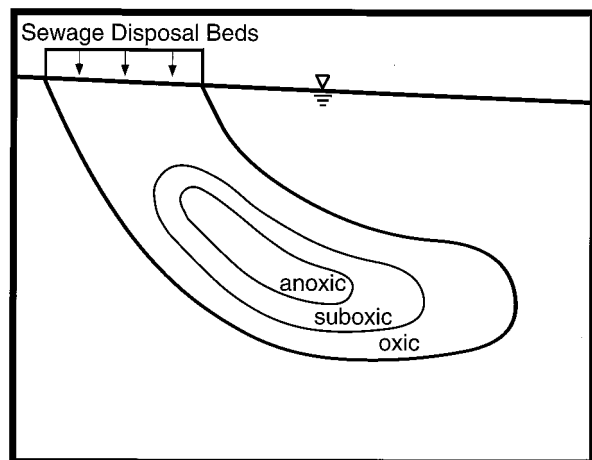


**Figure 1.** Conceptual illustration of redox zones in a vertical slice down the long profile of the plume at the Cape Cod site, oriented along a hypothetical flow plane.

duction, and (5) zone of methane production. Each zone is a result of oxidation of organic matter by the oxidant that will yield the greatest free energy change per mole of organic carbon oxidized [Champ *et al.*, 1979; Froelich *et al.*, 1979]. When this oxidant is depleted, the next most efficient oxidizer is used until there is no more organic carbon or oxidants left.

Three different redox zones have been identified within the sewage plume at the U.S. Geological Survey's Cape Cod research site in Massachusetts; i.e., oxic, suboxic, and anoxic zones [LeBlanc, 1984; Kent *et al.*, 1994]. It should be pointed out that neither sulfide nor methane have been observed at the Cape Cod site, even though sulfate is present. The anoxic zone at Cape Cod does contain dissolved iron; thus the most relevant redox reactions are oxygen reduction, denitrification, manganese reduction, and iron reduction [Smith and Duff, 1988; Smith *et al.*, 1991; Kent *et al.*, 1994]. The term "suboxic" is applied to the zone of denitrification and manganese reduction because of the persistence of small concentrations of dissolved oxygen. Figure 1 is a conceptualization of what the redox zones look like in a vertical slice through the long profile of the Cape Cod site aquifer, oriented along a hypothetical flow plane.

## 1.2. Simulation Approaches

Many models have been developed in an effort to characterize and simulate solute transport coupled with either biodegradation, redox processes, or general chemical reactions. Most models that address redox problems focus on biodegradation; Essaid *et al.* [1995] provide an excellent review. With models of this type, when more than one substrate or more than one process is involved, an empirical inhibition factor [Kindred and Celia, 1989; Essaid *et al.*, 1995] or a switching function [Kinzelbach *et al.*, 1991; Schäfer and Therrien, 1995] is needed. These parameters inhibit a reaction that yields a lower free energy change from occurring in the presence of a reaction that yields a higher free energy change. For example, denitrification is inhibited by the presence of appreciable dissolved oxygen.

While the inhibition factor and switching functions may seem to satisfy the thermodynamic criteria (i.e., free energy constraints), there is no theoretical basis for calculating either; they are fitting parameters. The microbial population that

dominates in a given situation, and thus the chemical reactions that dominate in a given situation, is a function of the amount of Gibbs free energy that can be liberated via microbially mediated chemical reactions. The more free energy released by a reaction, the higher the substrate consumption efficiency of the microbial population that is catalyzing the reaction. Thus it is logical to incorporate thermodynamics when considering biodegradation problems in which more than one substrate or redox process (e.g., more than one microbial population or more than one electron acceptor) is involved. If one writes out the complete chemical reaction for one or more biodegradation process, the free energy change associated with each reaction (i.e., the equilibrium constant) will dictate which reactions are feasible under which chemical conditions and no inhibition factor or switching function is required. There is no mathematical limit to the number of chemical reactions that can be included in such a model. An added bonus to this approach is that the concentrations of reaction products, as well as reactants, can be easily calculated.

In theory, the coupling of groundwater flow, solute transport, and geochemical reactions is rather straightforward. Reactive transport models that can include the necessary chemical reactions have been described in the literature [e.g., Liu and Narasimhan, 1989a, b; Yeh and Tripathi, 1990, 1991; Engesgaard and Kipp, 1992; Lichtner, 1992; McNab and Narasimhan, 1994; Steefel and Lasaga, 1994; Walter *et al.*, 1994a, b; Van Cappellan and Gaillard, 1996; Wunderly, 1996]. In practice, however, the large difference in energy yield between the various redox reactions leads to seriously ill-posed numerical problems. The thermodynamic equilibrium constants for redox reactions, which are functions of their energy yield, span tens of orders of magnitude. This leads to a chemical system in which concentrations, the dependent variables, range from their maximum field value to infinitesimally small. The result is the creation of extremely ill-conditioned Jacobian matrices when the commonly used Newton-Raphson method is employed.

The notion of "redox zones" leads to the idea that when attempting to simulate solute transport and chemical reactions in such aquifers, perhaps it is possible to ignore certain reactions under certain conditions. If this is true, then it follows that the range of values in subsequent Jacobians will be much smaller. This in turn leads to systems of equations that are much more numerically stable. Techniques such as basis switching improve numerical stability by rewriting chemical reactions in terms of dominant species, without altogether eliminating insignificant reactions [Lichtner, 1992; Bethke, 1996; Steefel and Yabusaki, 1996]. In this paper, we describe a method of compartmentalizing the dominant redox reactions that allows us to embed thermodynamics within a kinetic framework without encountering the numerical problems created by using thermodynamics. Our method can reduce the number of transport equations that need to be solved in space and time by reducing the number of chemical entities under consideration. In our ongoing work, we couple the reaction network for the development of redox zones to a model of subsurface fluid flow and solute transport for the Cape Cod site. Our new method facilitates (1) further understanding of redox processes, both organic and inorganic and (2) an ability to test hypotheses for processes that have occurred, and are occurring, at many field sites.

## 2. Model Development and Applications

### 2.1. Chemical Reactions

The basic strategy for solving geochemical problems numerically is straightforward. Mass action expressions are first written for each chemical reaction. Together with mass balance equations and charge balance equations (implicit or explicit) these equations constitute a system of  $N$  nonlinear equations in  $N$  unknowns. This system of equations is typically solved using the Newton-Raphson method. There are, however, nuances to the particular way in which redox reactions are written. More specifically, the issue is how the concentration of electrons ( $[e^-]$ ) is treated mathematically. *Liu and Narasimhan* [1989a] provide a thorough review of the five most common methods for treating redox reactions. In general, each of these five methods uses a redox parameter that describes the redox state or redox potential (e.g.,  $pE$ , where  $pE = -\log [e^-]$ ) of the geochemical system. When redox parameters are used, redox reactions are written as half reactions (i.e., one half reaction representing oxidation and another representing reduction, rather than one overall reaction representing the coupled chemical process).

It is possible to include  $[e^-]$  in the set of unknowns, but the numerics are arduous because  $[e^-]$  can easily span 20 orders of magnitude or more. In addition, there are two other, more significant conceptual problems when  $[e^-]$  is an unknown. Free, or aqueous, electrons do not exist in solution. If  $[e^-]$  is an unknown, then in a solute transport framework, electrons, or another variable representing the redox state of the water, must be transported; this is conceptually incorrect. Second, it is well known that there is no true  $pE$  for a natural water. The platinum electrode, which is widely used for field determinations of redox potential, is insensitive to many important redox couples [Stumm and Morgan, 1981]. Calculated  $pE$  values are representative of equilibrium among redox couples, a situation that is rarely achieved in nature [Lindberg and Runnells, 1984; Liu and Narasimhan, 1989a]. For example, values of  $pE$  for the suboxic zone of the sewage plume at the Cape Cod site, calculated from the concentrations of various redox sensitive constituents, range from 5.5 to 14.1 [Kent et al., 1994].

The conceptual difficulties with using  $pE$  or another variable representing the redox state motivated us to use an approach without such a variable. In our approach, all redox reactions are written as full reactions with an electron donor (i.e., dissolved organic carbon in this paper) coupled explicitly to an electron acceptor. *Lichtner* [1992], for example, used a similar approach for handling redox reactions. In this manner, we are not forced to calculate values for hypothetical chemical entities, nor are we confined to imposing an indeterminate property, such as  $pE$ , on the geochemical system.

We hypothesized a reaction network (see Appendix A) to represent the major geochemical processes that lead to the development of the three redox zones at the Cape Cod site. These processes are oxygen reduction, denitrification, manganese reduction, and iron reduction. Appendix B shows how the mass balance equations were formulated using values from the Cape Cod field data. Aqueous complexes that contributed <1% to the mass balance of the relevant component and solids that are undersaturated were deleted from the reaction network. The mass action and mass balance equations provide the 17 nonlinear algebraic equations necessary to solve for the 17 unknowns in this example.

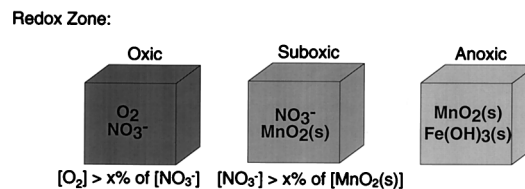


**Figure 2.** The boxes correspond to the zones used in our compartmentalized approach. Each compartment is defined by two redox reactions. Only one compartment is active at a time. The criteria that must be satisfied for a compartment to be active are shown, where  $X$  is the cutoff value for switching between compartments. When neither criterion is satisfied, only the anoxic compartment is active.

### 2.2. Compartmentalized Approach

**2.2.1. Description.** We have discussed the numerical difficulties that occur when, for example, all the reactions shown in Appendix A are included in a simulation. The numerical instability can be circumvented to some degree by making good initial guesses for the dependent variables. These difficulties are apparent in batch simulations but are even more apparent in the context of solute transport because the entire range of possible concentrations will be encountered at one time or another during the course of a transient solute transport simulation. This makes the selection of good initial guesses throughout a spatial and temporal domain difficult, since the extent of reaction cannot be known a priori. In addition, if all reactions are included, a larger number of transport equations is needed.

Redox zones can be defined by the redox sensitive species and thus the redox reactions that dominate. Therefore it is reasonable to assume that there are always some redox reactions that dominate over others and that some redox reactions can be ignored under certain conditions without incurring significant error. *Keating* [1995] used a technique in which all potential redox reactants are present initially, but certain redox reactions are removed from the reaction set if the concentrations of relevant reactants becomes limiting. We hypothesize that we can develop “compartments,” analogous to redox zones, in which each compartment contains the dominant redox reactions within its respective zone, but all potential redox reactions do not need to be included initially. The compartments have no spatial context, they should be thought of as different stages in reaction progress.

For the current example, there are two redox reactions in each compartment (Figure 2). The decision to switch from one compartment, or stage, to the next is based upon the relative proportion of the most energetic oxidant with respect to the least energetic oxidant in that compartment. For example, the reaction network for the compartment representing the oxic zone will be used until the concentration of dissolved oxygen is less than a specified percent of the available nitrate. When this occurs, the reaction network representing the suboxic zone will be used until the concentration of nitrate is less than a specified percent of the available manganese oxide. At this point, the reaction network for the compartment representing the anoxic zone will be used. The decision variable for switching (i.e., the cutoff value), does not need to be the same for switching between compartments two and three as it is for switching between compartments one and two.

Reactions that occur in compartments one and two affect

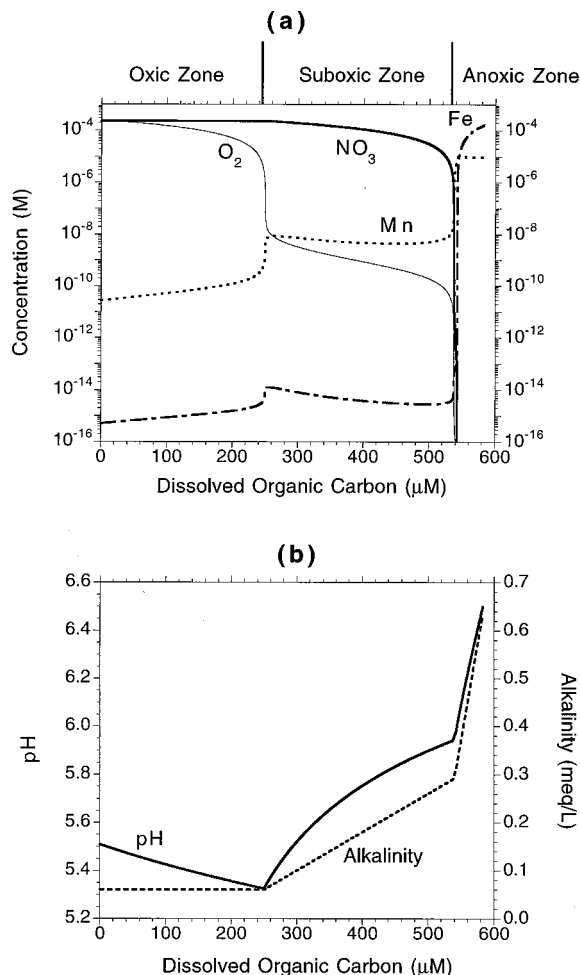


**Figure 3.** Distribution diagram generated without reaction compartmentalization showing (a) concentrations of redox sensitive species and (b) pH and alkalinity as a function of DOC reacted. The oxidic, suboxic, and anoxic zones are also shown.

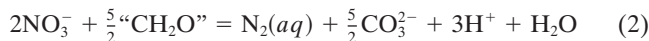
the chemistry of compartments two and three, respectively, and all the compartments use different components, species, and reaction sets. Thus information that is specific to a given reaction network (e.g., mass balances) is “lost” upon the switch between compartments. Therefore the “lost” information must be passed to the next compartment to update the initial conditions for the next reaction network. In contrast with techniques such as basis switching [e.g., *Bethke*, 1996], no chemical reactions need to be rewritten and no equilibrium constants need to be altered; insignificant reactions are merely dropped from the reaction network as new ones are added.

**2.2.2. Test problem.** We developed a batch simulation problem against which to test the compartmentalized approach. The test problem is based upon representative conditions at the Cape Cod site. We first solved the test problem without compartmentalizing the reactions, i.e., all the reactions shown in Appendix A are used in each redox zone and all 17 equations shown in Appendix B are solved simultaneously during the entire course of the simulation. The initial conditions (i.e., the known quantities), derived from field data, are also shown in Appendix B. The results for the test problem without reaction compartmentalization are shown in Figure 3, which was generated with HYDRAQL [*Papelis et al.*, 1988], a descen-

dent of MINEQL [*Westall et al.*, 1976]. Figure 3a shows the distribution of redox sensitive species and the development of redox zones as a function of the amount of DOC reacted, as predicted by thermodynamics. Figure 3b shows the changes in pH and alkalinity as the simulation proceeds. The simulation results in Figure 3 were realized with some difficulty. To construct the first portion of the diagram, from 0 μM DOC to ~540 μM, required DOC increments of 10<sup>-1</sup> μM to ensure convergence (10<sup>3</sup> titration steps to react 100 μM of DOC). Beyond 540 μM (i.e., the anoxic/iron zone) the required DOC step to ensure convergence was 10<sup>-4</sup> μM (i.e., 10<sup>6</sup> titration steps to react 100 μM of DOC).

**2.2.3. Application of the compartmentalized approach to the test problem.** Our implementation of the compartmentalized approach to solve the test problem uses HYDRAQL to simulate the simplified reaction networks within each compartment (see Appendix A and Figure 2).

As an example of switching between compartments, consider the switch from compartment one (oxic) to compartment two (suboxic). Here we only show the redox reactions in each compartment and do not show the contribution of individual chemical species to the mass balance of each component. For compartment one, we have two redox reactions, one representing aerobic respiration and the other representing denitrification. The components are H<sup>+</sup>, CO<sub>3</sub><sup>2-</sup>, NO<sub>3</sub><sup>-</sup>, and “CH<sub>2</sub>O”, where “CH<sub>2</sub>O” is a surrogate representing all the reactive DOC:



The mass balance equations are

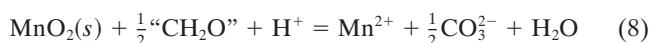
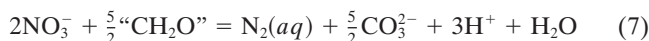
$$T_{\text{H}^+}^1 = -\text{ALK} + 2[\text{CO}_2]_T + 2[\text{O}_2]_T \quad (3)$$

$$T_{\text{CO}_3^{2-}}^1 = [\text{CO}_2]_T + [\text{O}_2]_T \quad (4)$$

$$T_{\text{NO}_3^-}^1 = [\text{NO}_3^-]_T \quad (5)$$

$$T_{\text{“CH}_2\text{O”}}^1 = [\text{“CH}_2\text{O”}]_T - [\text{O}_2]_T \quad (6)$$

where  $T_i$  is the total analytical concentration of each component. The components in compartment two are H<sup>+</sup>, CO<sub>3</sub><sup>2-</sup>, NO<sub>3</sub><sup>-</sup>, Mn<sup>2+</sup>, and “CH<sub>2</sub>O.” Aerobic respiration no longer occurs and manganese reduction has been added:



The mass balance equations (i.e., as if there never were a compartment one) are

$$T_{\text{H}^+}^2 = -\text{ALK} + 2[\text{CO}_2]_T - [\text{MnO}_2(s)]_T \quad (9)$$

$$T_{\text{CO}_3^{2-}}^2 = [\text{CO}_2]_T + 0.5[\text{MnO}_2(s)]_T \quad (10)$$

$$T_{\text{NO}_3^-}^2 = [\text{NO}_3^-]_T \quad (11)$$

$$T_{\text{Mn}^{2+}}^2 = [\text{MnO}_2(s)]_T \quad (12)$$

$$T_{\text{“CH}_2\text{O”}}^2 = [\text{“CH}_2\text{O”}]_T - 0.5[\text{MnO}_2(s)]_T \quad (13)$$

If there is a switch from compartment one to compartment two, then the mass balance equations for compartment two

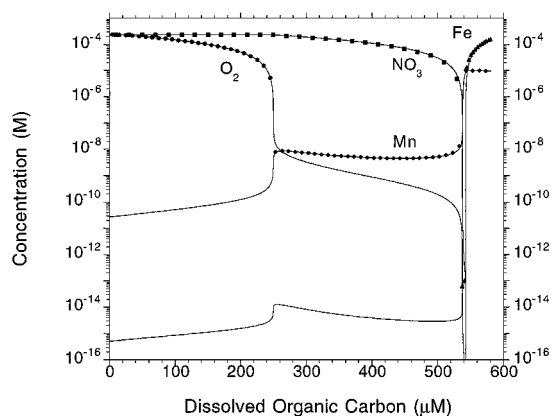


**Figure 4.** Comparison of 1% cutoff (plot symbols) with results shown in Figure 3. Only a portion of the symbols are plotted, to avoid clutter. The sequence of symbols truncates as a function of the cutoff value. In a qualitative sense the agreement is nearly perfect.

must be modified to account for the effects of the compartment one reactions on the chemistry of compartment two. This prevents the reaction information of compartment one from being lost:

$$T_{\text{H}^+}^{2 \text{ modified}} = T_{\text{H}^+}^2 + 2 * ([\text{O}_2] \text{ used in compartment 1}) \quad (14)$$

$$T_{\text{CO}_3^{2-}}^{2 \text{ modified}} = T_{\text{CO}_3^{2-}}^2 + 1 * ([\text{O}_2] \text{ used in compartment 1}) \quad (15)$$

$$T_{\text{NO}_3^-}^{2 \text{ modified}} = [\text{NO}_3]_T \quad (16)$$

$$T_{\text{Mn}^{2+}}^{2 \text{ modified}} = [\text{MnO}_2(\text{s})]_T \quad (17)$$

$$T_{\text{CH}_2\text{O}^-}^{2 \text{ modified}} = T_{\text{CH}_2\text{O}^-}^2 + 1.25 * ([\text{NO}_3^-] \text{ used in compartment 1}) - 1 * ([\text{O}_2] \text{ remaining in compartment 1}) \quad (18)$$

The results from the compartmentalized simulation, using a cutoff value of 1% for both instances of compartmental switching, are plotted in Figure 4 as an overlay on top of Figure 3a (we consider Figure 3a to be the correct answer). Clearly, the match between the simulation approaches is nearly perfect; differences are not discernible when plotted in this manner. This result is pleasing, but a rigorous statistical evaluation is more appropriate than a simple visual comparison. To do this, five model performance evaluation statistics, shown in Table 1, were used to quantitatively evaluate the compartmentalized approach against the model that includes all redox reactions all the time. Note that although the root-mean-square error (in percent) is quite high for Mn and Fe, the other statistics appear to have reasonably good values. The results are also plotted in the scatterplots shown in Figure 5. To address the problems encountered with a cutoff value of 1%, we tested the impact of a lower cutoff value (0.01%) for both instances of compartmental switching. The scatterplots (Figure 5) and statistical values (Table 1) demonstrate the effectiveness of our procedure when the more appropriate cutoff value is used. Note that in the anoxic zone, where the smallest DOC increments were needed to construct Figure 3a (i.e.,  $10^{-4} \mu\text{M}$ ), we were able to use DOC increments as large as  $10^{-1} \mu\text{M}$  with the compartmentalized approach, without encountering convergence problems.

### 2.3. Kinetic Framework

**2.3.1. Description.** Thermodynamics provides the driving force for simulating the geochemical reactions that represent biodegradation. Clearly, consideration of these reactions as equilibrium reactions is inappropriate because they represent biologic processes, which do not occur instantaneously. Furthermore, for the redox reactions under consideration, equilibrium lies extremely far to the right, as the reactions are written (Appendix A). So even if these reactions were occurring in very slowly moving groundwater, rate limitations are needed because there is no “dynamic” equilibrium among re-

**Table 1.** Statistical Values for Two Different Cutoff Criteria

Sample Size <i>n</i> and Model Performance Statistics	O <sub>2</sub>	NO <sub>3</sub>	Mn	Fe	pH	ALK	Perfect Model
<i>Cutoff = 1%</i>							
<i>n</i>	2479	5353	3329	455	5808	5808	
ME	0.0000	0.0000	0.0000	0.0000	0.0342	0.0000	0.0000
RMSE, %	0.0000	0.7596	40.7861	12.6620	0.1625	3.2810	0.0000
CD	1.0000	0.9821	0.9556	0.9171	0.9588	0.9400	1.0000
EF	1.0000	0.9997	0.9760	0.9726	0.9987	0.9983	1.0000
CRM	0.0000	0.0056	-0.0532	-0.1183	-0.0009	-0.0146	0.0000
<i>Cutoff = 0.01%</i>							
<i>n</i>	2514	5378	3318	454	5832	5832	
ME	0.0000	0.0000	0.0000	0.0000	0.0001	0.0000	0.0000
RMSE, %	0.0000	0.0011	0.0006	0.0000	0.0002	0.0013	0.0000
CD	1.0000	1.0000	1.0000	1.0000	0.9999	1.0000	1.0000
EF	1.0000	1.0000	1.0000	1.0000	1.0000	1.0000	1.0000
CRM	0.0000	0.0000	0.0000	0.0000	0.0000	0.0000	0.0000

Changing the cutoff from 1% to 0.01% results in significant improvement in model performance (e.g., root-mean-square error (RMSE) for Mn improved from 40.786% to 0.0006% with the change in tolerance). The model performance statistics used here are described by *Loague and Green* [1991]. The lower limit for the maximum error (ME), RMSE, and coefficient of determination (CD) statistics is zero. The maximum value for modeling efficiency (EF) is one. Both EF and coefficient of residual mass (CRM) can become negative. If EF is less than zero, the compartmentalized approach values are worse than simply using the mean of the standard modeling approach results. Several of the statistics are sensitive to a few large values.

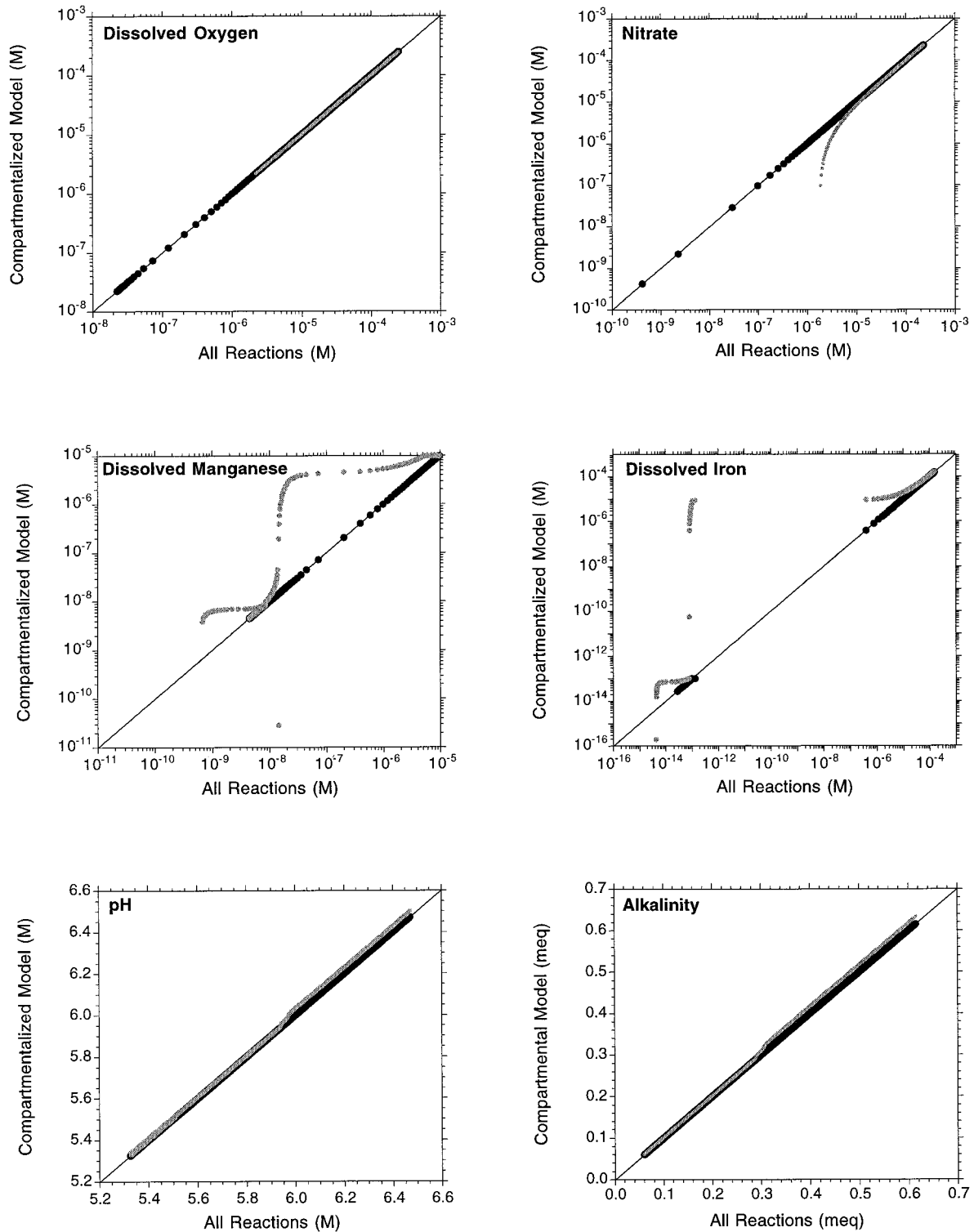


**Figure 5.** Scatterplot comparing the compartmentalized approach with the approach in which all reactions are used in each redox zone. Results with a cutoff value of 1% (gray plot symbols) and 0.01% (black plot symbols) are shown.

actants and products; these reactions only proceed in the forward direction (i.e., to the right, as written).

There are several kinetic formulations for biogeochemical reactions reported in the literature [e.g., see *Essaid et al.*, 1995]. Some of these kinetic formulations incorporate microbial dynamics while others do not. Two biogeochemical formulations,

Monod and Michaelis-Menten, are mathematically similar except that the former has a term for the concentration of microbes while the latter does not (i.e., the Michaelis-Menten form is appropriate for situations in which there is no net microbial growth). Both the Monod and Michaelis-Menten expressions reduce to first-order kinetics at low reactant con-

centrations and to zero-order kinetics at high reactant concentrations. The relatively low DOC concentrations at the Cape Cod site [Thurman *et al.*, 1986] suggest that there is no net growth of the bacterial communities. Data from laboratory experiments using materials from the Cape Cod site have been successfully modeled with the Michaelis-Menten expression (R. L. Smith, personal communication, 1997). In addition, data from denitrification tracer tests at the Cape Cod site have been successfully modeled using zero-order kinetics [Smith *et al.*, 1996]. For these reasons, we use Michaelis-Menten kinetics in our ongoing work with coupled solute transport/geochemical simulations (for process-based modeling). We use zero-order kinetics for model development with the batch simulations that are reported in this paper:

$$dC/dt = -k \quad (19)$$

where  $C$  is the concentration of any reactant,  $t$  is time, and  $k$  is the rate constant. The zero-order kinetic formulation is used solely for simplicity; any rate expression can be used in our model.

In the absence of thermodynamic constraints, Monod kinetics, Michaelis-Menten kinetics,  $n$ th-order kinetics, and kinetic expressions based on microscopic reversibility may incorrectly simulate reaction progress if two or more kinetic reactions are present in a reaction set. The simulated kinetic reactions will proceed as a function of time regardless of the geochemical conditions, potentially allowing thermodynamically infeasible reactions to occur. This is why inhibition factors and switching functions have been used. The approach we use here is to use thermodynamics to determine reaction feasibility and the relative amount of DOC that should be apportioned to the feasible reactions, and kinetic expressions to limit reaction progress. Our method contrasts with that of Keating [1995], who used a strictly equilibrium formulation for all chemical reactions and a time-dependent source of electrons to control the progress of redox reactions.

As an example, consider the oxic compartment, where oxygen reduction and denitrification can occur and denitrification represents the lower-energy reaction. In our model, each reaction can be assigned a different rate, but for the sake of this description, let us assume that (1) the two redox reactions proceed at the same rate, (2) oxygen and nitrate concentrations are initially the same, and (3) DOC is present in excess (i.e., the time step is small enough so that all the available DOC is not reacted within one time step). The third assumption is important because it ensures that the oxygen concentration (in this example) will not be artificially large because of DOC limitations.

According to kinetics (i.e., without any form of reaction suppression), at the end of a time step a certain amount of DOC will have reacted, reducing the concentrations of oxygen and nitrate equally and leaving some free DOC unreacted. Since the system is not DOC limited, we assume that the kinetically derived concentration of oxygen is correct but that the kinetically derived concentration of nitrate must be checked for thermodynamic feasibility. To do this, a thermodynamic (i.e., equilibrium) simulation is performed in which enough DOC is added to the system to lower the oxygen concentration to the same value as the kinetically derived concentration. If the same amount of DOC that was consumed by oxygen in the kinetic simulation is required, then thermodynamics indicates that the denitrification reaction should be completely suppressed under the specified geochemical condi-

tions. If more DOC is required, then denitrification is only partially suppressed. In either case, if the concentration of nitrate is higher in the thermodynamic simulation, then the kinetic simulation is incorrect and the thermodynamic result is used. If the concentration of nitrate in the thermodynamic simulation is equal to or lower than the kinetic simulation, then the kinetic simulation is correct and it is used.

### 2.3.2. Incorporation of the compartmentalized approach.

We incorporated the compartmentalized approach within a kinetic framework to simulate the development of redox zones as a function of time in a batch system. We adapted KEMOD [Yeh *et al.*, 1993], the mixed kinetic equilibrium geochemistry module of HYDROGEOCHEM 2.1 [Yeh and Salvage, 1995], to perform the kinetic and thermodynamic calculations according to the procedure described above. The basic numerical solution strategy for KEMOD is similar to that of HYDRAQL [Papelis *et al.*, 1988] and MINEQL [Westall *et al.*, 1976], except that KEMOD has the ability to include elementary kinetic reactions based upon microscopic reversibility. We modified KEMOD so that it could solve irreversible,  $n$ th order kinetics. The reactions used are shown in Appendix A. In the kinetic framework, however, all four redox reactions are treated as irreversible, zero-order kinetic reactions that proceed from left to right, as written. The  $pH$  buffering and speciation reactions are treated as equilibrium reactions. The initial conditions and equations are the same as those shown in Appendix B, except for the addition of equations of the form of (19) to represent the rate limitations imposed on the redox reactions. The kinetic equations are not used for the thermodynamic calculation, and the mass action equations (for the redox reactions) are not used for the kinetic calculation. In addition, DOC is present in excess over the concentrations of all the redox sensitive reactants. Thermodynamics would thus predict instant utilization and exhaustion of all redox reactants.

Since reaction progress is limited by kinetic constraints, the redox reactants are not exhausted immediately but rather the redox zones develop as a function of time. No inhibition factors or switching functions are used to suppress reactions. Redox reactions that are in the same compartment can both occur simultaneously if the geochemical conditions are appropriate (e.g., under low oxygen but relatively higher nitrate concentrations). If the geochemical conditions are not appropriate for simultaneous redox reactions, the lower-energy reaction is automatically suppressed by the thermodynamic constraints. There is always overlap between sequential redox reactions (e.g., denitrification can occur in the oxic and suboxic compartments).

The results from the kinetic/thermodynamic simulation are plotted in Figure 6 as a function of dimensionless time. The simulation was run from an initial condition of  $pH$  5.5 to a final  $pH$  of 6.5, as in Figure 3. The curves in Figure 6 truncate abruptly due to compartmental switching (i.e., the cutoff criteria are enforced). The development of redox zones as a function of time is clearly shown. Throughout the reaction space, lower-energy redox reactions are suppressed by higher-energy redox reactions due to the thermodynamic constraints. Reaction progress is limited by the kinetic constraints.

## 3. Discussion

### 3.1. Impact of Cutoff Value

The results shown in Table 1 and Figure 5 clearly illustrate the impact the cutoff value has on the compartmentalized

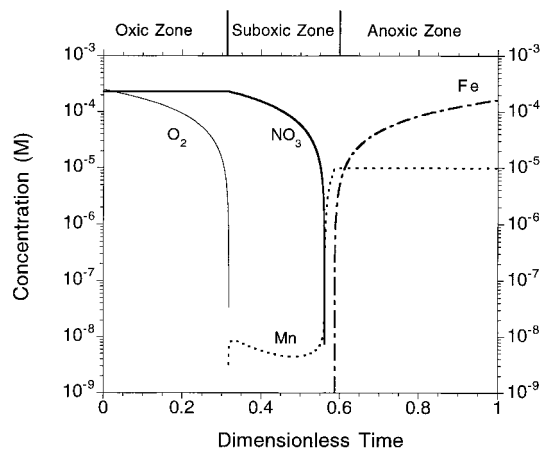


**Figure 6.** Development of redox zones and distribution of redox sensitive species as a function of time. Suppression of lower-energy reactions is accomplished through thermodynamic constraints.

simulations. Overall, the match between the two methods we compare is very good, as shown in Figure 4. The trends are matched precisely, and, from the point of view of Figure 4 (cutoff = 1%), there does not appear to be any cause for concern. However, when the results are plotted as scatterplots, errors become apparent for the simulation that uses a 1% cutoff value. In itself, this is not necessarily a problem. It depends on what the goals of the simulations are. If one is interested in general trends in the development of redox zones, then a cutoff value of 1% is probably fine. If, however, one is interested in tracking a particular chemical entity, then the ability to simulate its appearance/disappearance with reasonable accuracy is highly dependent on the cutoff value.

The best cutoff value for a particular situation is dependent on a number of factors, including the use of different redox reactions (e.g., using different organic compounds instead of solely using "CH<sub>2</sub>O" to represent all of the available DOC). For instance, the free energy yield associated with the degradation of, say, toluene, may produce curves with different slopes. These slopes may also be different for different oxidants. In general, however, there is a correlation between desired accuracy and magnitude of the cutoff value; smaller cutoff values yield more accurate results. There is a trade-off, however, between lower cutoff values (i.e., more accuracy) and simulation time. We made no attempt to determine the optimal cutoff value for the system we studied. Such an optimal value would be a function of DOC increment size, desired accuracy, initial conditions, and the reactions under consideration.

### 3.2. Impact of Site-Specific Geochemical Assumptions

Characteristics of the redox boundaries shown in Figures 3 and 6 depend upon assumptions made about the initial conditions and the free energy of the solids. Free energies of hydrous ferric oxide and manganese oxide were taken from published compilations [Morel and Hering, 1993]. Iron and manganese oxides on aquifer sediments from the Cape Cod site exist as complex hydroxypolymer coatings; the actual free energies are unknown and iron and manganese likely exist as solids with a range of compositions [Coston *et al.*, 1995]. Inclusion of a range of compositions for each class of solids would

affect overall reactivity, which would affect the minimum computed concentrations of dissolved iron and dissolved manganese and the positions of the redox boundaries. Maximum computed concentrations of dissolved iron and dissolved manganese depend on the initial conditions.

Characteristics of the evolution of *pH* and alkalinity shown in Figure 3 also depend on site-specific geochemical assumptions. Stoichiometric coefficients for both the hydrogen ion and carbonate species in the redox reactions differ somewhat for different organic compounds. Thus use of different organic compounds in the computations would yield different *pH* and alkalinity trajectories. Inclusion of *pH* buffers in addition to those of the carbonate species would also influence the *pH* trajectory. Surface complexation reactions between surface sites on the aquifer sediments and hydrogen ions would provide additional *pH* buffering [Stollenwerk, 1995]. The result of additional buffers would be that greater quantities of organic matter and electron donors would be required to achieve the *pH* values characteristic of each of the redox zones.

### 3.3. Comparison With Field Observations

The simulations reported here were performed over the *pH* range 5.5–6.5 to represent the range of field conditions from pristine groundwater to the average conditions found in the core of the upgradient portion of the sewage plume at the Cape Cod site. Qualitatively, the simulation results agree with field observations as can be seen by comparing Figures 3 and 6 with Figure 7. The simulation results in Figures 3a and 6 show the presence of an oxidic zone with high concentrations of dissolved oxygen and nitrate, a suboxic zone with high concentrations of nitrate and elevated dissolved manganese, and an anoxic zone with high concentrations of dissolved manganese and dissolved iron. Figure 3b shows the increases in *pH* associated with the suboxic and anoxic zones as seen in Figure 7.

The theoretically based equilibrium constants, which represent the Gibbs free energy of reaction, determine the most favorable reactions. For example, in the *pH* range observed at the Cape Cod site, our thermodynamically based model predicts that iron reduction will not commence, and thus no iron zone will form, until all of the available manganese has been reduced. This is because the energy released by manganese reduction is so much greater than the energy released by iron reduction. A similar situation is described by Chapelle and Lovley [1992] in which sulfate reduction was observed only after ferric iron was depleted.

The simulation results shown in Figures 3 and 6 represent what would occur in a batch system. Figure 7 represents one snapshot in time of a vertical profile, at one location, in the transient Cape Cod groundwater flow system. As such, the simulation results are only comparable to field data in a qualitative sense. Figure 7 may, however, represent a steady state in which concentrations are not changing with time, even though thermodynamic equilibrium is not achieved. This could occur because reactants and products are constantly flowing in and out of any given control volume. Thus a quantitative model evaluation against field data can only be realized in the context of solute transport simulations, which is the next phase of this study.

### 3.4. Simultaneous Occurrence of Redox Reactions

An important aspect of any model that simulates sequential, microbially mediated redox reactions is the recognition that under certain geochemical conditions, competing reactions

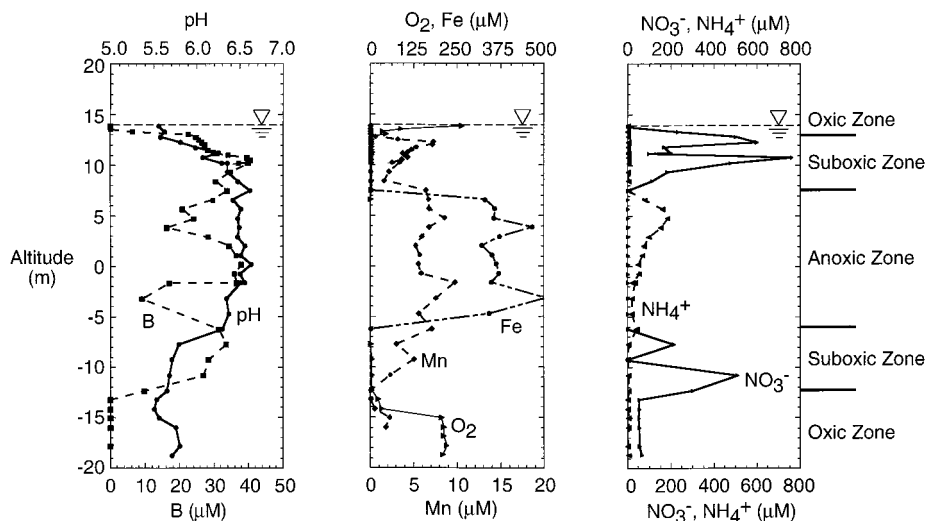


**Figure 7.** Concentration versus depth profiles showing the redox zones at the Cape Cod site (modified from Kent *et al.* [1994]).

may occur simultaneously (e.g., incomplete suppression of a lower-energy reaction). Our method allows for this possibility by always having at least two redox reactions in each compartment and by overlapping reactions between compartments (e.g., denitrification is included in the oxic, and suboxic compartments and manganese reduction is included in the suboxic and anoxic compartments).

Figure 6 shows, for example, denitrification and manganese reduction occurring simultaneously in the micromolar range. The time over which this occurs appears to be rather small, but this is a function of the kinetic formulation (i.e., zero-order kinetics). If first-order kinetics were used in the low concentration ranges, as it is with Michaelis-Menten kinetics, the time over which simultaneous redox reactions occur would be greater.

#### 4. Conclusions

Redox zones often develop in contaminated aquifers as a response to microbes oxidizing dissolved organic carbon coupled to the reduction of the electron acceptor that yields the greatest amount of free energy. Thermodynamics provides a basis for predicting under what conditions a given reaction, or microbial process, will occur. With this tool, the development of redox zones can be simulated on a firm theoretical basis, rather than in a framework in which calibration must be done empirically (e.g., inhibition factors). Furthermore, the qualitative description of sequential redox reactions and development of redox zones can be quantified using thermodynamics.

The large difference in energy yields between the various redox reactions leads to systems of equations that are ill-conditioned. We have circumvented this difficulty by developing a rational method to eliminate insignificant reactions while maintaining the integrity of the numerical solution. We did this by compartmentalizing the reaction networks in a manner that is conceptually based on the redox zones themselves. We focus on the reactions that give rise to a particular zone, while those that are not important, due to reactant availability and energetic efficiency, are ignored. When the cutoff criteria are selected appropriately (i.e., the switch between compartments is

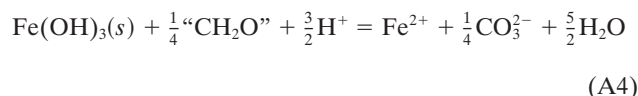
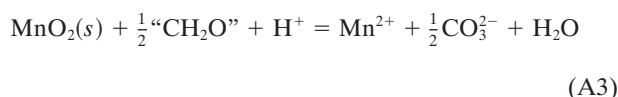
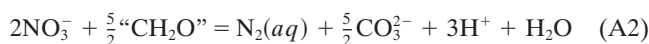
done properly), no significant errors are generated. In addition, it is possible to reduce the number of transport equations required to simulate solute transport coupled with geochemical reactions.

When the compartmentalized approach is placed within a kinetic framework, the development of redox zones can be simulated as a function of time. Our method of incorporating kinetics allows the use of any kinetic formulation to constrain reaction progress, while still using thermodynamics to prevent reactions from occurring under infeasible conditions. The compartmentalized approach lays the foundation for the next phase of our ongoing work, in which we couple the reaction network for the development of redox zones to a model of subsurface fluid flow and solute transport for the Cape Cod site.

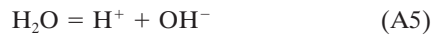
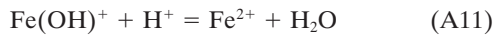
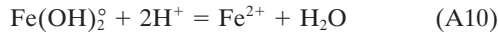
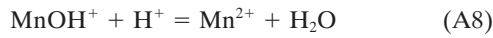
#### Appendix A

Below is the reaction network used to simulate the development of redox zones and evaluate the compartmentalized approach.

##### A1. Redox Reactions



The oxic compartment contains reactions (A1) and (A2). The suboxic compartment contains reactions (A2) and (A3). The anoxic compartment contains reactions (A3) and (A4).

**A2. The pH Buffering Reactions****A3. Aqueous Speciation Reactions****Appendix B: Equations and Initial Conditions Used for Model Evaluation****B1. Mass Action Equations**

$$[\text{O}_2(aq)] = [\text{CO}_3^{2-}][\text{H}^+]^2[{}^{\circ}\text{CH}_2\text{O}^{-}]^{-1}10^{-68.38}$$

$$[\text{NO}_3^-] = ([\text{N}_2(aq)][\text{CO}_3^{2-}]^{2.5}[\text{H}^+]^3[{}^{\circ}\text{CH}_2\text{O}^{-}]^{-2.5}10^{-163.5})^{0.5}$$

$$[\text{Mn}^{2+}] = [\text{CO}_3^{2-}]^{-0.5}[\text{H}^+][{}^{\circ}\text{CH}_2\text{O}^{-}]^{0.5}10^{32.84}$$

$$[\text{Fe}^{2+}] = [\text{CO}_3^{2-}]^{-0.25}[\text{H}^+]^{1.5}[{}^{\circ}\text{CH}_2\text{O}^{-}]^{0.25}10^{11.92}$$

$$[\text{H}^+] = [\text{OH}^-]^{-1}10^{-13.99}$$

$$[\text{H}_2\text{CO}_3] = [\text{CO}_3^{2-}][\text{H}^+]^210^{6.35}$$

$$[\text{HCO}_3^-] = [\text{CO}_3^{2-}][\text{H}^+]10^{10.32}$$

$$[\text{MnOH}^+] = [\text{Mn}^{2+}][\text{H}^+]^{-1}10^{-10.0}$$

$$[\text{MnHCO}_3^+] = [\text{Mn}^{2+}][\text{CO}_3^{2-}][\text{H}^+]10^{-12.1}$$

$$[\text{Fe}(\text{OH})_2^0] = [\text{Fe}^{2+}][\text{H}^+]^{-2}10^{-20.57}$$

$$[\text{Fe}(\text{OH})^+] = [\text{Fe}^{2+}][\text{H}^+]^{-1}10^{-9.5}$$

**B2. Mass Balance Equations**

$$\begin{aligned} T_{\text{H}^+} &= [\text{H}^+] - [\text{OH}^-] + 2[\text{H}_2\text{CO}_3] + [\text{HCO}_3^-] + 2[\text{O}_2(aq)] \\ &\quad - 3[\text{N}_2(aq)] - [\text{MnO}_2(s)] - 1.5[\text{Fe}(\text{OH})_3(s)] \\ &\quad - [\text{MnOH}^+] + [\text{MnHCO}_3^+] - 2[\text{Fe}(\text{OH})_2^0] - [\text{Fe}(\text{OH})^+] \\ &= -\text{ALK} + 2[\text{CO}_2]_T + 2[\text{O}_2]_T - [\text{MnO}_2(s)]_T \\ &\quad - 1.5[\text{Fe}(\text{OH})_3(s)]_T \end{aligned}$$

where ALK is the carbonate alkalinity and  $T_i$  is the total analytical concentrations of each model component.

$$\begin{aligned} T_{\text{CO}_3^{2-}} &= [\text{CO}_3^{2-}] + [\text{H}_2\text{CO}_3] + [\text{HCO}_3^-] + [\text{O}_2(aq)] \\ &\quad - 2.5[\text{N}_2(aq)] + 0.5[\text{MnO}_2(s)] \\ &\quad + 0.25[\text{Fe}(\text{OH})_3(s)] + [\text{MnHCO}_3^+] \\ &= [\text{CO}_2]_T + [\text{O}_2]_T + 0.5[\text{MnO}_2(s)]_T \\ &\quad + 0.25[\text{Fe}(\text{OH})_3(s)]_T \end{aligned}$$

$$T_{\text{NO}_3^-} = [\text{NO}_3^-] + 2[\text{N}_2(aq)] = [\text{NO}_3^-]_T$$

$$\begin{aligned} T_{\text{Mn}^{2+}} &= [\text{Mn}^{2+}] + [\text{MnO}_2(s)] + [\text{MnOH}^+] + [\text{MnHCO}_3^+] \\ &= [\text{MnO}_2(s)]_T \end{aligned}$$

$$\begin{aligned} T_{\text{Fe}^{2+}} &= [\text{Fe}^{2+}] + [\text{Fe}(\text{OH})_3(s)] + [\text{Fe}(\text{OH})_2^0] + [\text{Fe}(\text{OH})^+] \\ &= [\text{Fe}(\text{OH})_3(s)]_T \end{aligned}$$

$$\begin{aligned} T_{\text{CH}_2\text{O}^{\circ}} &= [{}^{\circ}\text{CH}_2\text{O}^{\circ}] - [\text{O}_2(aq)] + 2.5[\text{N}_2(aq)] \\ &\quad - 0.5[\text{MnO}_2(s)] + 0.25[\text{Fe}(\text{OH})_3(s)] \\ &= [{}^{\circ}\text{CH}_2\text{O}^{\circ}]_T - [\text{O}_2]_T - 0.5[\text{MnO}_2(s)]_T \\ &\quad - 0.25[\text{Fe}(\text{OH})_3(s)]_T \end{aligned}$$

**B3. Initial Conditions, Derived From Field Data ( $M$ )**

$$\text{ALK} = 6 \times 10^{-5}$$

$$[\text{CO}_2]_T = 5 \times 10^{-4}$$

$$[\text{O}_2]_T = 2.5 \times 10^{-4}$$

$$[\text{NO}_3^-]_T = 2.3 \times 10^{-4}$$

$$[\text{MnO}_2(s)]_T = 1 \times 10^{-5}$$

$$[\text{Fe}(\text{OH})_3(s)]_T = 1 \times 10^{-3}$$

$$[{}^{\circ}\text{CH}_2\text{O}^{\circ}]_T = 0$$

**Acknowledgments.** This work was supported by a U.S. Environmental Protection Agency STAR Graduate Fellowship (U 914715-01-2) to RHA and grants to KL from the National Science Foundation (EAR-9506467-001), the Western Region Hazardous Substance Research Center (SU95-5), and the University of California Center for Water Resources (SA6070). Reviews and comments by Carl Steefel, Barbara Bekins, Ken Stollenwerk, and the anonymous *Water Resources Research* reviewer greatly improved earlier versions of this manuscript. We wish to thank Denis LeBlanc, Kathryn Hess, Jennifer Savoie, Kimberly Campo, and Timothy McCobb of the U.S. Geological Survey, Massachusetts, for their expertise and assistance. We are also grateful to Garrison Sposito, Mark Reed, and George Parks for insightful discussions regarding this work.

**References**

- Baedecker, M. J., and W. Back, Hydrogeological processes and chemical reactions at a landfill, *Ground Water*, 15(5), 429–437, 1979a.
- Baedecker, M. J., and W. Back, Modern marine sediments as a natural analog to the chemically stressed environment of a landfill, *J. Hydrology*, 43, 393–414, 1979b.
- Baedecker, M. J., I. M. Cozzarelli, R. P. Eganhouse, D. I. Siegel, and P. Bennett, Crude oil in a shallow sand and gravel aquifer, III, Biogeochemical reactions and mass balance modeling in anoxic groundwater, *Appl. Geochem.*, 8, 569–586, 1993.
- Barcelona, M. J., T. R. Holm, M. R. Schock, and G. K. George, Spatial and temporal gradients in aquifer oxidation-reduction conditions, *Water Resour. Res.*, 25, 991–1003, 1989.
- Bennett, P. C., D. I. Siegel, M. J. Baedecker, and M. F. Hult, Crude oil in a shallow sand and gravel aquifer, I, Hydrogeology and inorganic geochemistry, *Appl. Geochem.*, 8, 529–549, 1993.
- Bethke, C. M., *Geochemical Reaction Modeling*, Oxford Univ. Press, New York, 1996.
- Champ, D. R., J. Gullens, and R. E. Jackson, Oxidation-reduction sequences in ground water flow systems, *Can. J. Earth Sci.*, 16, 12–23, 1979.
- Chapelle, F. H., and D. R. Lovley, Competitive exclusion of sulfate reduction by Fe(III)-reducing bacteria: A mechanism for producing discrete zones of high-iron ground water, *Ground Water*, 30(1), 29–36, 1992.
- Coston, J. A., C. C. Fuller, and J. A. Davis, Pb<sup>2+</sup> and Zn<sup>2+</sup> adsorption by a natural Al- and Fe-bearing surface coating on an aquifer sand, *Geochim. Cosmochim. Acta*, 59(17), 3535–3547, 1995.
- Cozzarelli, I. M., M. J. Baedecker, R. P. Eganhouse, and D. F. Goerlitz, The geochemical evolution of low-molecular-weight organic

- acids derived from the degradation of petroleum contaminants in groundwater, *Geochim. Cosmochim. Acta*, 58(2), 863–877, 1994.
- Edmunds, W. M., A. H. Bath, and D. L. Miles, Hydrochemical evolution of the East Midlands Triassic sandstone aquifer, England, *Geochim. Cosmochim. Acta*, 46, 2069–2081, 1982.
- Edmunds, W. M., D. L. Miles, and J. M. Cook, A comparative study of sequential redox processes in three British aquifers, in *Hydrochemical Balances of Freshwater Systems*, edited by E. Eriksson, pp. 55–72, IAHS—AISH, Uppsala, Sweden, 1984.
- Eganhouse, R. P., M. J. Baedecker, I. M. Cozzarelli, G. R. Aiken, K. A. Thorn, and T. F. Dorsey, Crude oil in a shallow sand and gravel aquifer, II, Organic geochemistry, *Appl. Geochem.*, 8, 551–567, 1993.
- Engesgaard, P., and K. L. Kipp, A geochemical transport model for redox-controlled movement of mineral fronts in groundwater flow systems: A case of nitrate removal by oxidation of pyrite, *Water Resour. Res.*, 28, 2829–2843, 1992.
- Essaid, H. I., B. A. Bekins, E. M. Godsy, E. Warren, M. J. Baedecker, and I. M. Cozzarelli, Simulation of aerobic and anaerobic biodegradation processes at a crude oil spill site, *Water Resour. Res.*, 31, 1995.
- Froelich, P. N., G. P. Klinkhammer, M. L. Bender, N. A. Luedtke, G. R. Heath, D. Cullen, P. Dauphin, D. Hammond, B. Hartman, and V. Maynard, Early oxidation of organic matter in pelagic sediments of the eastern equatorial Atlantic: suboxic diagenesis, *Geochim. Cosmochim. Acta*, 43, 1075–1090, 1979.
- Jackson, R. E., and R. J. Patterson, Interpretation of pH and Eh trends in a fluvial-sand aquifer system, *Water Resour. Res.*, 18, 1255–1268, 1982.
- Keating, E. H., Reactive transport modeling: An application to redox geochemistry of groundwater discharging to a stream in northern Wisconsin, Ph.D. thesis, Univ. of Wisc., Madison, 1995.
- Kent, D. B., J. A. Davis, L. C. D. Anderson, B. A. Rea, and T. D. Waite, Transport of chromium and selenium in the suboxic zone of a shallow aquifer: Influence of redox and adsorption reactions, *Water Resour. Res.*, 30, 1099–1114, 1994.
- Kindred, J. S., and M. A. Celia, Contaminant transport and biodegradation, 2, Conceptual model and test simulations, *Water Resour. Res.*, 25, 1149–1159, 1989.
- Kinzelbach, W., W. Schäfer, and J. Herzer, Numerical modeling of natural and enhanced denitrification processes in aquifers, *Water Resour. Res.*, 27, 1123–1135, 1991.
- LeBlanc, D. R., Sewage plume in a sand and gravel aquifer, Cape Cod, Massachusetts, *U.S. Geol. Surv. Water Supply Pap.*, 2218, 28 pp., 1984.
- Lichtner, P. C., Time-space continuum description of fluid/rock interaction in permeable media, *Water Resour. Res.*, 28, 3135–3155, 1992.
- Lindberg, R. D., and D. D. Runnells, Ground water redox reactions: An analysis of equilibrium state applied to Eh measurements and geochemical modeling, *Science*, 225, 925–927, 1984.
- Liu, C. W., and T. N. Narasimhan, Redox-controlled multiple-species reactive chemical transport, 1, Model development, *Water Resour. Res.*, 25, 869–882, 1989a.
- Liu, C. W., and T. N. Narasimhan, Redox-controlled multiple-species reactive chemical transport, 2, Verification and application, *Water Resour. Res.*, 25, 883–910, 1989b.
- Loague, K., and R. E. Green, Statistical and graphical methods for evaluating solute transport models: Overview and application, *J. Contam. Hydrol.*, 7, 261–283, 1991.
- Lovley, D. R., F. H. Chappelle, and J. C. Woodward, Use of dissolved H<sub>2</sub> concentrations to determine distribution of microbially catalyzed redox reactions in anoxic groundwater, *Environ. Sci. Technol.*, 28(7), 1205–1210, 1994.
- Lyngkilde, J. L. and T. H. Christensen, Redox zones in a landfill leachate pollution plume (Vejen, Denmark), *J. Contam. Hydrol.*, 10(4), 273–289, 1992.
- McNab, W. W., and T. N. Narasimhan, Modeling reactive transport of organic compounds in groundwater using a partial redox disequilibrium approach, *Water Resour. Res.*, 30, 2619–2635, 1994.
- Morel, F. M. M., and J. G. Hering, *Principles and Applications of Aquatic Chemistry*, John Wiley, New York, 1993.
- Papelis, C., K. F. Hayes, and J. O. Leckie, HYDRAQL: A program for the computation of chemical equilibrium composition of aqueous batch systems including surface-complexation modeling of ion adsorption at the oxide/solution interface, *Stanford Univ. Dep. Civ. Eng. Tech. Rep.*, 306, 130 pp., 1988.
- Schäfer, W., and R. Therrien, Simulating transport and removal of xylene during remediation of a sandy aquifer, *J. Contam. Hydrol.*, 19, 205–236, 1995.
- Smith, R. L., and J. H. Duff, Denitrification in a sand and gravel aquifer, *Appl. Environ. Microbiol.*, 54(5), 1071–1078, 1988.
- Smith, R. L., B. L. Howes, and J. H. Duff, Denitrification in nitrate-contaminated groundwater: Occurrence in steep vertical geochemical gradients, *Geochim. Cosmochim. Acta*, 55, 1815–1825, 1991.
- Smith, R. L., S. P. Garabedian, and M. H. Brooks, Comparison of denitrification activity measurements in groundwater using cores and natural-gradient tracer tests, *Environ. Sci. Tech.*, 30(12), 3448–3456, 1996.
- Steeffel, C. I., and A. C. Lasaga, A coupled model for transport of multiple chemical species and kinetic precipitation/dissolution reactions with application to reactive flow in single phase hydrothermal systems, *Am. J. Sci.*, 294, 529–592, 1994.
- Steeffel, C. I., and S. B. Yabusaki, OS3D/GIMRT: Software for multicomponent-multidimensional reactive transport: User manual and programmer's guide, *Rep. PNL-11166*, Pac. Northwest Lab., 1996.
- Stollenwerk, K. G., Modeling the effects of variable groundwater chemistry on adsorption of molybdate, *Water Resour. Res.*, 31, 347–357, 1995.
- Stumm, W., and J. J. Morgan, *Aquatic Chemistry*, John Wiley, New York, 1981.
- Thurman, E. M., L. B. Barber, and D. R. LeBlanc, Movement and fate of detergents in groundwater: A field study, *J. Contam. Hydrol.*, 1, 143–161, 1986.
- Van Cappellan, P., and J-F Gaillard, Biogeochemical dynamics in aquatic sediments, in *Reactive Transport in Porous Media*, *Rev. Mineralog.*, vol. 34, edited by P. C. Lichtner, C. I. Steffel, and E. H. Oelkers, pp. 335–375, Mineralog. Soc. of Am., Washington, D. C., 1996.
- Walter, A. L., E. O. Frind, D. W. Blowes, C. J. Ptacek, and J. W. Molson, Modeling multicomponent reactive transport in groundwater, 1, Model development and evaluation, *Water Resour. Res.*, 30, 3137–3148, 1994a.
- Walter, A. L., E. O. Frind, D. W. Blowes, C. J. Ptacek, and J. W. Molson, Modeling multicomponent reactive transport in groundwater, 2, Metal mobility in aquifers impacted by acidic mine tailings discharge, *Water Resour. Res.*, 30, 3149–3158, 1994b.
- Westall, J. C., J. L. Zachary, and F. M. M. Morel, MINEQL: A computer program for the calculation of the chemical equilibrium composition of aqueous systems, *Tech. Note 18*, Ralph M. Parsons Lab, Mass. Inst. of Technol., Cambridge, Mass., 1976.
- Wunderly, M. D., D. W. Blowes, E. O. Frind, and C. J. Ptacek, Sulfide mineral oxidation and subsequent reactive transport of oxidation products in mine tailings impoundments: A numerical model, *Water Resour. Res.*, 32, 3173–3187, 1996.
- Yeh, G. T., and K. Salvage, HYDROGEOCHEM 2.1: A coupled model of hydrologic transport and geochemistry with both equilibrium and kinetic reactions, technical rep. Penn State Univ. Dep. of Civ. and Environ. Eng., State College, 1995.
- Yeh, G. T., and V. S. Tripathi, HYDROGEOCHEM: A coupled model of hydrological and geochemical equilibrium of multicomponent systems, *Rep. ORNL-6371*, Oak Ridge Natl. Lab., Oak Ridge, Tenn., 1990.
- Yeh, G. T., and V. S. Tripathi, A model for simulating transport of reactive multispecies components: Model development and demonstration, *Water Resour. Res.*, 27, 3075–3094, 1991.
- Yeh, G. T., G. Iskra, J. M. Zachara, and J. E. Szecsody, KEMOD: A mixed chemical kinetic and equilibrium model of complexation, adsorption, ion-exchange, precipitation/dissolution, redox, and acid-base reactions, technical report, Penn State Univ. Dep. of Civ. and Environ. Eng., State College, 1993.

R. H. Abrams and K. Loague, Department of Geological and Environmental Sciences, Stanford University, Stanford, CA 94305-2115. (e-mail: abrams@pangea.stanford.edu)

D. B. Kent, U.S. Geological Survey, 345 Middlefield Road, MS 465, Menlo Park, 94025.

(Received August 25, 1997; revised February 4, 1998; accepted February 6, 1998.)

